Supporting Information

(111) Facet-engineered SnO_2 as Electron Transport Layer for Efficient and Stable Perovskite Solar Cells

Keshav Kumar Sharma, Rohit, Sochannao Machinao, and Ramesh Karuppannan

Department of physics, Indian Institute of Science, Bangalore 560012, Karnataka, India

Corresponding Author: kramesh@iisc.ac.in

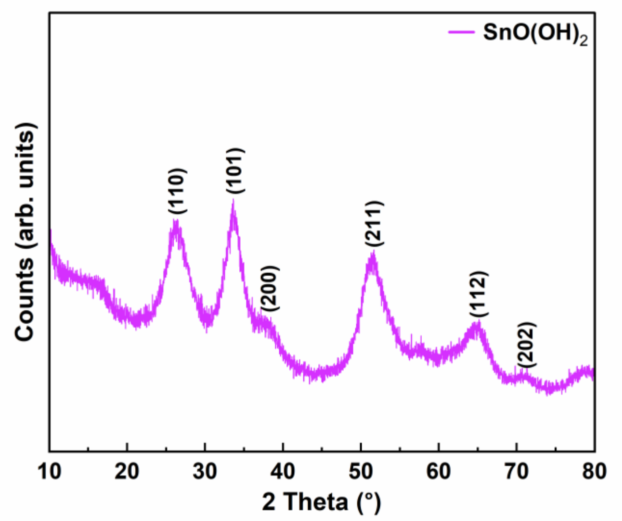

Fig. S1 XRD pattern of $SnO(OH)_2$ powder[1,2] extracted from SnO_2 precursor at 120 °C.

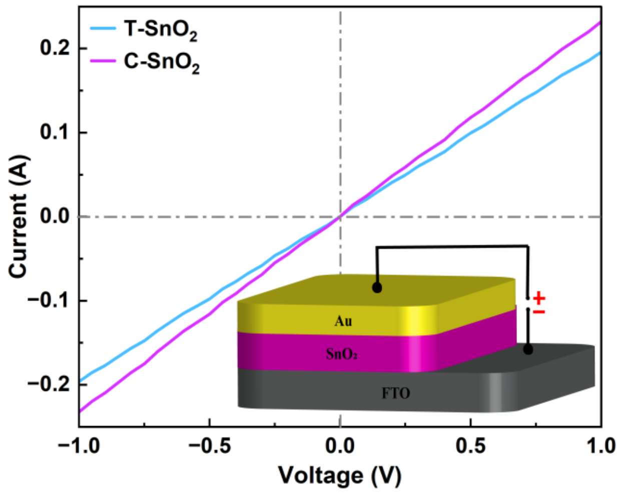

Fig. S2 I-V curves of the T-SnO_2 and C-SnO_2 thin films.

The optical band gap of the the T-SnO_2, C-SnO_2 and CsFAMA films are calculated using the UV-vis spectra fit to tauc equation[3]

$$(\alpha h\nu)^n = A(h\nu - E_g)$$

Where α is the absorption coefficient calculated as $\alpha = 2.303\frac{A}{d} = -2.303\frac{1}{d}log\frac{1}{T}$, A is the absorbance, T is the transmittance and d is the thickness of the film. The optical band gap of the T-SnO_2, C-SnO_2 and CsFAMA films are calculated to 4.01, 4.10 and 1.61 eV, respectively (Fig. 2d & S2).

The valance band maximum (E_v) was determined by the following equation[4]

$$E_v = (E_{cutoff} - HOS) - h\nu$$

The E_{cutoff} and HOS (higheat occupied state) positions are indicated in Fig. 2e & S2. As expacted, the E_v values of the T-SnO_2, C-SnO_2 and CsFAMA films are calculated to be -8.10, -8.04 and -5.40 eV, respectively.

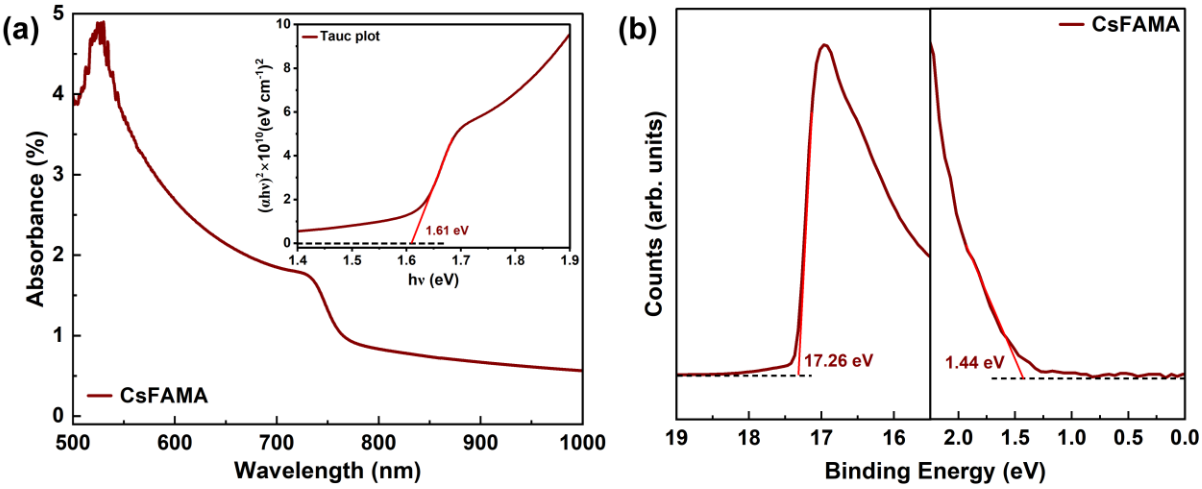

Fig. S3 UV-vis absorption spectrum and UPS spectrum of CsFAMA film.

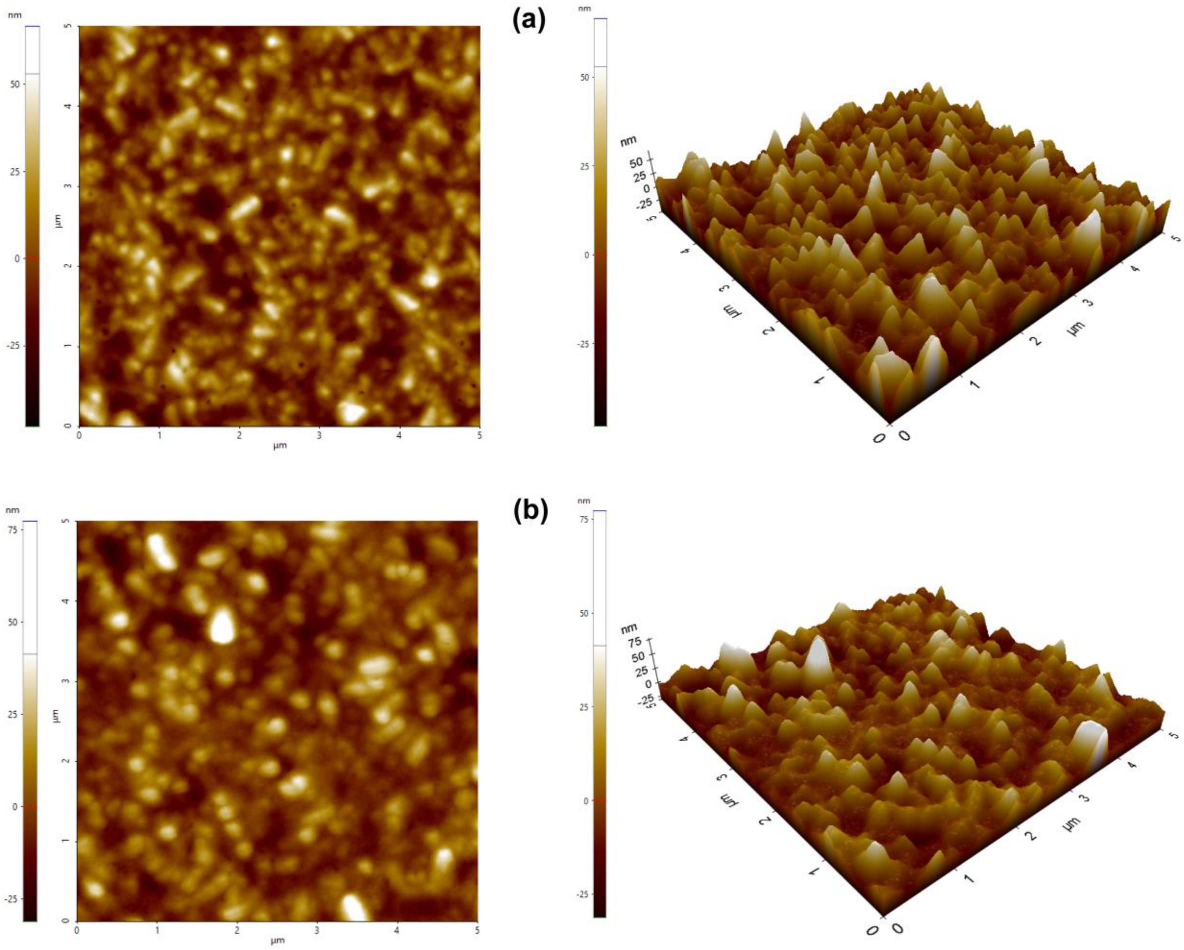

Fig. S4 The 2d and 3d AFM images of (a) T-SnO_2 and (b) C-SnO_2 thin film on FTO coated glass substrate.

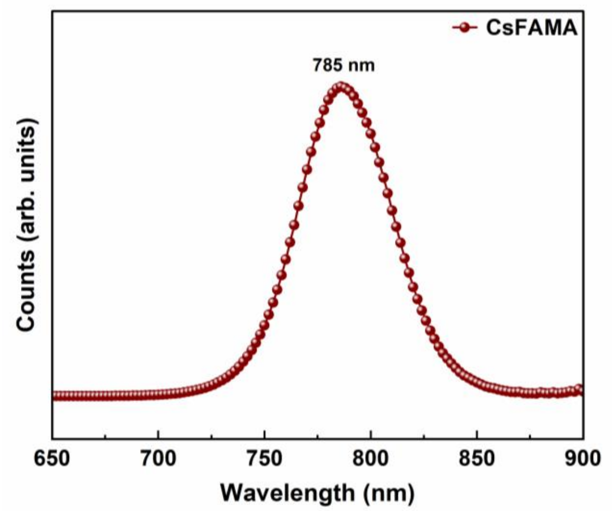

Fig. S5 PL spectrum of pristine CsFAMA film.

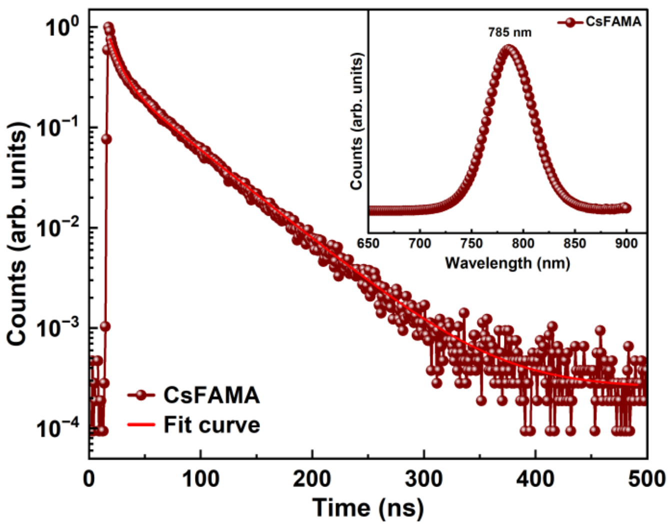

Fig. S6 TRPL spectrum of pristine CsFAMA film.

Table S1: The fitting parameters of TRPL spectra

Sample	A_1	τ_1(ns)	A_2	τ_2 (ns)	A_3	τ_3 (ns)	τ_{ave} (ns)
CsFAMA	0.57	4.70	0.42	41.42	-	-	36.53
T-SnO_2/CsFAMA	0.95	1.23	0.04	6.38	0.007	29.07	5.52
C-SnO_2/CsFAMA	0.79	0.63	0.04	3.79	0.005	17.49	3.28

The average lifetime was determined by the following equation[5]

$$< \tau_{ave} >= \frac{\sum_{i=1,2,3} A_i \tau_i^2}{\sum_{i=1,2,3} A_i \tau_i}$$

where A_i is the pre-exponential factor and τ_i is the average lifetime.

Table S2: The parameters of the SCLC for different electron-only devices.

Sample	V_{TFL} (V)	N_{trap} (cm^{-3})
T-SnO_2	0.564	1.80×10^{16}
C-SnO_2	0.445	1.42×10^{16}

The density of trap states was calculated using the following equation[6]

$$N_{trap} = \frac{2\varepsilon_r \varepsilon_0 V_{TFL}}{eL^2}$$

where $V_{TFL}$is the trap filling limit voltage, L is the thickness of the perovskite layer, ε_r is the relative dielectric constant of the perovskite layer ($\varepsilon_r \approx 26$), ε_0 is the vacuum dielectric constant, and *e* is the amount of electric charge.

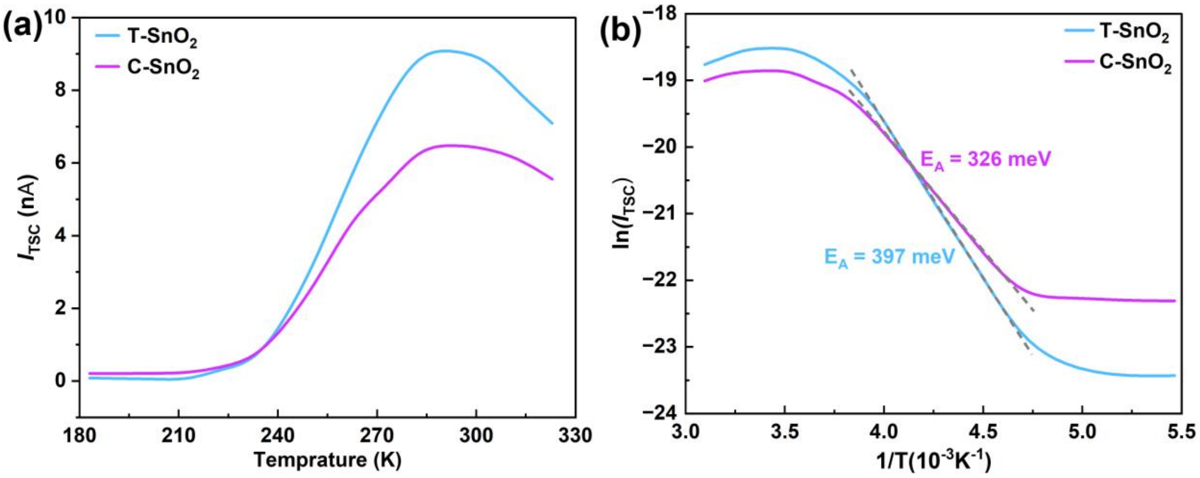

Fig, S7 (a) TSC profile of PSCs, and (b) Arrhenius plot obtained from the TSC profile with different ETLs in PSCs. Each dashed line represents the slope of the profile.

To understand the recombination process in the PSC with C-SnO_2 ETL, we conducted thermally stimulated current (TSC) analysis (see Fig. S7a). The activation energy of the trap states was calculated from the slope of the Arrhenius plot (see Fig. S7b) of the TSC profile, using the following relation[7]

$$I_{TSC} \propto \exp\left(-\frac{E_A}{k_B T}\right)$$

where E_A, k_B, and T are the activation energy, Boltzmann constant, and temperature, respectively.

Table S3: *J–V* data of 30 independent devices.

T-SnO_2	V_{OC} (V)	J_{SC} ($mA.cm^{-2}$)	FF (%)	PCE (%)	C-SnO_2	V_{OC} (V)	J_{SC} ($mA.cm^{-2}$)	FF (%)	PCE (%)
1	1.08	23.67	76.5	19.64	**1**	1.10	23.89	77.3	20.34
2	1.08	23.53	76.3	19.38	**2**	1.10	23.76	76.9	20.09
3	1.07	23.87	75.8	19.36	**3**	1.10	23.89	75.3	19.78
4	1.09	23.69	74.1	19.13	**4**	1.11	23.54	75.6	19.75
5	1.08	23.45	74.3	18.81	**5**	1.10	23.48	76.3	19.70
6	1.07	23.58	73.8	18.62	**6**	1.10	23.64	75.1	19.53
7	1.08	23.33	72.9	18.55	**7**	1.10	23.67	74.9	19.50
8	1.07	23.68	73.2	18.54	**8**	1.09	23.93	74.7	19.48
9	1.08	23.33	73.1	18.42	**9**	1.10	23.83	74.3	19.47
10	1.06	23.59	73.3	18.33	**10**	1.11	23.06	75.5	19.32
11	1.07	23.47	72.6	18.24	**11**	1.11	23.23	74.8	19.29
12	1.06	23.77	72.3	18.22	**12**	1.10	23.63	74.2	19.28
13	1.06	23.46	72.5	18.03	**13**	1.11	23.14	74.8	19.21
14	1.07	23.11	72.1	17.83	**14**	1.09	23.67	74.0	19.06
15	1.06	23.34	71.6	17.72	**15**	1.10	23.46	73.6	18.99
16	1.05	23.53	71.5	17.66	**16**	1.09	23.46	73.3	18.74
17	1.07	23.48	70.3	17.67	**17**	1.08	23.54	73.5	18.68
18	1.06	23.41	70.7	17.55	**18**	1.10	23.14	73.1	18.61
19	1.06	23.64	69.5	17.42	**19**	1.11	23.06	72.6	18.58
20	1.08	23.45	68.5	17.35	**20**	1.09	23.34	72.9	18.54
21	1.07	23.61	68.4	17.28	**21**	1.09	23.27	72.8	18.46
22	1.07	23.27	69.1	17.21	**22**	1.08	23.45	72.6	18.38
23	1.06	23.64	66.9	16.76	**23**	1.11	22.86	72.3	18.34

24	1.05	24.34	64.7	16.54	**24**	1.10	23.56	70.3	18.21
25	1.06	23.71	67.1	16.87	**25**	1.09	23.85	69.1	17.96
26	1.06	23.49	66.1	16.46	**26**	1.10	23.66	68.3	17.76
27	1.06	23.12	66.3	16.24	**27**	1.09	24.14	66.2	17.42
28	1.08	22.76	64.2	15.78	**28**	1.10	23.87	65.4	17.18
29	1.05	23.22	64.6	15.75	**29**	1.10	23.36	65.8	16.90
30	1.05	23.05	63.6	15.39	**30**	1.08	23.06	65.3	16.26

References

1 S. Khalameida, M. Samsonenko, J. Skubiszewska-Zięba and O. Zakutevskyy, *Adsorpt. Sci. Technol.*, 2017, **35**, 853–865.

2 C. Akyil, G. Akdas, P. Afsin and M. Ürgen, *Mater. Chem. Phys.*, 2019, **221**, 263–271.

3 K. Kranthiraja, M. Parashar, R. K. Mehta, S. Aryal, M. Temsal and A. B. Kaul, *Sci. Rep.*, 2022, **12**, 18574.

4 X. Wu, Y. Jiang, C. Chen, J. Guo, X. Kong, Y. Feng, S. Wu, X. Gao, X. Lu, Q. Wang, G. Zhou, Y. Chen, J. Liu, K. Kempa and J. Gao, *Adv. Funct. Mater.*, , DOI:10.1002/adfm.201908613.

5 X. Hao, Y. Fan, W. Deng and Z. Jin, *Carbon N. Y.*, 2024, **218**, 118752.

6 Q. Geng, S. Zhang, H. Sui, X. Liu, Y. Li, H. Zhong, C. Yao, Q. Zhang and X. Chu, *ACS Appl. Mater. Interfaces*, 2024, **16**, 38124–38133.

7 D. Koo, Y. Choi, U. Kim, J. Kim, J. Seo, E. Son, H. Min, J. Kang and H. Park, *Nat. Nanotechnol.*, , DOI:10.1038/s41565-024-01799-8.